JPE 13-3-18

http://dx.doi.org/10.6113/JPE.2013.13.3.497

Improvement of Available Battery Capacity in Electric Vehicles

Yow-Chyi Liu†

†Department of Electrical Engineering, Kao Yuan University, Kaohsiung, Taiwan

Abstract

This paper proposes a new method to improve the available battery capacity in electric vehicles by connecting lead-acid batteries with lithium-ion battery in parallel to supply power. In addition, this method combines the discharge characteristics of batteries to improve their efficiency and lower their cost for electric vehicles. A lithium-ion battery set is used to connect with *N* sets of lead-acid batteries in parallel. The lead-acid battery supplies the initial power. When the lead-acid battery is discharged by the load current until its output voltage drops to the cut-off voltage, the power management unit controls the lead-acid battery and changes it to discharge continuously with a small current. This discharge can be achieved by connecting the lead-acid battery to a lithium-ion battery in parallel to supply the load power or to discharge its current to another lead-acid or lithium-ion battery. Experimental results demonstrates that the available capacity can be improved by up to 30% of the rated capacity of the lead-acid batteries.

Key words: Available capacity, Battery efficiency, Electric vehicles, Lead-Acid battery, Lithium-Ion battery

I. INTRODUCTION

Battery cost and battery capacity are the key factors in determining whether electric vehicles can be used widely [1]. Batteries are currently more expensive than fuel, and limited mileage severely restricts the use of electric vehicles. These problems must be resolved in practical applications. Having a high energy density, lithium-ion batteries can improve the mileage range of electric vehicles, yet the battery cost remains high. Therefore, electric vehicle research focuses on simulatneously lowering battery costs and increasing efficiency. Although lead-acid batteries have a lower energy density than lithium-ion batteries, lead-acid batteries cost less.

As the voltage of a single battery is low, it is necessary to connect a number of batteries in series to supply power to meet the load voltage demand. Connecting batteries in parallel can increase both battery capacity and application flexibility. However, even if the same type of batteries are connected in parallel, circulating current may be generated due to the different internal impedance of the cells. Therefore, there is a need to overcome such circulating current problems [2]. There are studies indicating the exploration of intermittent current discharge methods using parallel-connected lithium-ion batteries to supply power. These research findings have shown that the intermittent current discharge method is able to release more capacity than constant current [3]-[5].

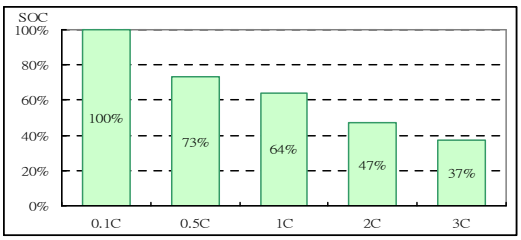

Fig. 1. The capacity of the CSB lead-acid battery.

As the available battery capacity is subject to the load current size, the releasable capacity varies under different discharge currents. For instance, while a larger discharge current implies a smaller battery released capacity, a smaller discharge current implies a larger battery released capacity. Such phenomena are especially obvious in lead-acid batteries. Fig. 1 shows the capacity of a CSB 4.5AH/12V lead-acid battery at different discharge rates [6]. When the output current is 0.5C, the available capacity of the lead-acid battery is 73% of its rated capacity. Additionally, a situation in which the output current is 1~2C reduces the available battery capacity to 64~47%.

Fig. 2 shows the capacity of a Molicel 2.9AH lithium-ion battery at different discharge rates [7]. When the output current

Manuscript received Aug. 17, 2012; revised Feb. 27, 2013
Recommended for publication Associate Editor Tae-Woong Kim.
†Corresponding Author: liuyc@cc.kyu.edu.tw
Tel: +886-7-6077285, Fax: +886-7-6077009, Kao Yuan University
Department of Electrical Engineering, Kao Yuan University, Taiwan

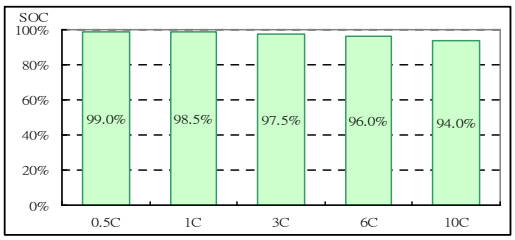

Fig. 2. The capacity of the Molicel lithium-ion battery.

is 0.5C, the available capacity of the lithium-ion battery is 99% of its rated capacity. When the output current is 1~2C, the available battery capacity is 97%. Lithium-ion batteries have excellent discharge characteristics, whereas the load current significantly impacts the capacity of lead-acid batteries. This paper focuses mainly on completely releasing the energy from a lead-acid battery.

II. BATTERY CAPACITY

Battery capacity information informs electric vehicle drivers of the current state of charge (SOC) to remain aware of the battery's remaining operational time and to estimate the mileage in order to determine when to charge the battery. Multiplying the battery residual capacity (Wh) with the energy consumption factor of an electric vehicle (km/Wh) allows drivers to accurately predict the mileage of electric vehicles based on the current battery capacity [8-10].

The power demand of electric vehicles can be divided into three modes: (1) Accelerating operation and uphill road mode, i.e. a large amount of power is required; (2) Constant speed operation mode, i.e. a lower amount of power is required; and (3) Decelerating operation and downhill road mode, i.e. it can deliver regenerated braking power. Despite consuming power in the first and second modes, an electric vehicle can recharge its battery in the third mode.

Estimating the battery capacity further allows electric vehicle drivers to avoid battery over-charging and over-discharging in order to extend the battery service life. The estimation methods of the battery residual capacity include the discharge test, open circuit voltage measurement, internal resistance measurement, coulometric measurement, loaded voltage measurement, electrolyte concentration measurement, the coup de fouet effect, peulert equation estimation, artificial neural networks, and fuzzy control [11-13]

III. THE PROPOSED METHOD

A. Configuration of the Parallel Battery

Various discharge currents will result in relatively large differences in the application efficiency of a battery. In most battery applications, when the battery has discharged until the output voltage reaches the drop cut-off voltage, there is still a large amount of energy that has not been released. To use the stored energy of a battery effectively, when a lead-acid battery has released a large amount of output current and reaches the cut-off voltage, the power supply is switched to the parallel-connected lithium-ion battery and the lead-acid batteries. At this point, by controlling the lead-acid battery to release a smaller output current to provide power to the load along with the parallel-connected lithium-ion battery, it is possible to increase the efficiency of the lead-acid battery.

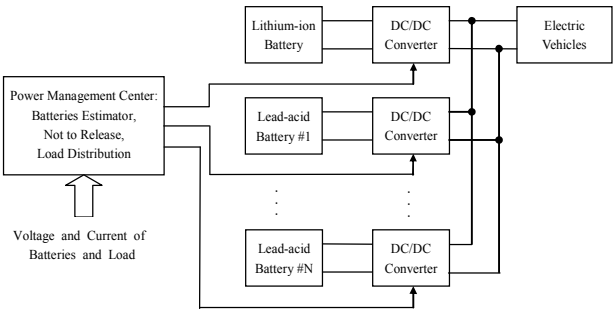

Fig. 3. The proposed configuration of the parallel power supply.

Fig. 3 illustrates the proposed configuration of the parallel power supply system for lead-acid batteries and a lithium-ion battery. The battery management center includes the estimation of battery capacity, the unreleased capacity and the load distribution. The voltage and current of the load, as well as the voltage and current of the lead-acid and lithium-ion batteries are measured. Additionally, each lead-acid battery is detected to determine whether its output voltage has reached the cut-off voltage. If it has, a re-use plan for the unreleased energy of the lead-acid battery is then conducted. Namely, a smaller output current (1C~0.1C) from this lead-acid battery is discharged until all of the stored energy of the battery has been released. It has been estimated that this capacity accounts for 30~50% of the rated power of lead-acid batteries.

The proposed parallel power supply initially allows the lead-acid battery to supply the power. When the lead-acid battery has discharged to the cut-off voltage, the power supply switches to the parallel-connected lithium-ion and lead-acid batteries. However, at this point, the output power from the lead-acid batteries must be controlled to release only a smaller amount of the discharged current. Since the output power from the lead-acid batteries is less than the power demand from the electric vehicle, the insufficient power is compensated for by the lithium-ion battery.

When the electric vehicle has stopped or reached its destination, the lead-acid battery continuously discharges a small amount of current to the lithium-ion battery. At this time, the lithium-ion battery is in the charging state. During the rest period of the electric vehicle, especially when it is waiting for a return trip, as much of the stored energy of the lead-acid battery as possible must be transferred to the lithium-ion battery in order to increase the energy of the lithium-ion battery.

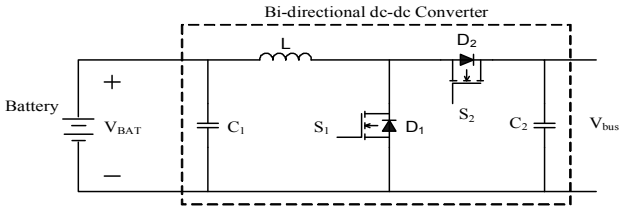

Fig. 4. A bi-directional dc-dc converter.

Doing so increases the efficiency of the lead-acid battery capacity.

B. Bi-directional DC-DC Converter

To ensure that the discharge action of the batteries is coming from the same group of dc converters, the bi-directional dc-dc converter shown in Fig. 4 is employed. The difference between a bi-directional converter and a general power converter is that there is no fixed output or input terminal in its circuit operation. It needs to follow the power flow direction to define its output and input positions. The application scope of a bi-directional converter includes electric vehicles, fuel cell systems, renewable energy conversion systems, etc [14-18].

In an electric vehicle system, for example, the regenerated brake energy can be used to perform battery charging through a bi-directional converter. When the electric vehicle is running under the motor status, the operation state of the bi-directional converter can be switched to the battery discharging state to provide the electric vehicle with the power it needs. As the bi-directional dc-dc converter is changed from a buck converter, changing the diode of the buck converter into an active power switch enables it to convert into the bi-directional mode.

The operation mode using the battery management center to control the bi-directional dc-dc converter can be divided into two types of operation modes. The first is the buck mode where the energy is delivered from the high-voltage side V_{bus} to the low-voltage side of the battery. Here, the bi-directional converter serves as a charger. The second type of operation mode is the boost mode where the output voltage from the lead-acid battery is raised to a required voltage for the load. In this case, the energy is delivered from the low-voltage side of the battery to the high-voltage side V_{bus} to supply power to the load.

When the bi-directional dc-dc converter operates in boost mode, the battery works as an input terminal, and the V_{bus} side works as an output terminal. Thus, the battery is in the discharge state. The battery energy is delivered to the V_{bus} side through the control of the on or off switch of S_1. When S_1 is on and S_2 is off, the energy from the input side is stored in inductor L and the load power is provided by capacitor C_2. When S_1 is off, diode D_2 is on to release the inductor energy to the V_{bus} side, and capacitor C_2 is in the charging state.

When the bi-directional dc-dc converter operates in buck mode, the V_{bus} side works as an input terminal, and the battery side works as an output terminal. Thus, the lead-acid batteries operate in the charging state. The energy from the V_{bus} side is used to charge the battery through the control of the on or off switch of S_2. When S_2 is on and S_1 is off, the energy from the input side is delivered to inductor L and the battery. When S_2 is off, the inductor current flows through diode D_1 and transfers the reserved energy from inductor L to the battery.

C. Analysis of the Voltage-Mode and Current-Mode Control

When the bi-directional dc-dc converter operates in boost mode, the energy saved in the battery can be provided to the load at the high voltage side. The high voltage side V_{bus} can be adjusted by controlling the discharge current of the battery. Take the voltage loop as the outer loop in order to adjust the output voltage to achieve the voltage regulation effect. In addition, take the current loop as the inner loop to speed up the transient response. This will improve system stability and provide over-current protection.

The discharge current command of the battery, I_{bat}* can be derived from the voltage regulation controller G_v via the errors between the voltage command V_{bus}* and the actual value I_{bat}*. This can be specified as Equation (1).

$$I_{bat}^{*} = G_v \times (V_{bus}^{*} - V_{bus}) \tag{1}$$

$$G_v = k_P + \frac{k_i}{s} \tag{2}$$

Equation (2) shows the voltage regulation controller G_v, where k_p and k_i are the proportion of the voltage regulation controller and the integral control gain, respectively.

Ignoring the internal resistance of inductor L and the consumption and voltage drop of the power semiconductor switch and introducing a current prediction method for current control to calculate the switch duty ratio via the current error value, forces the actual discharge current I_{bat} close to the discharge current command I_{bat}* under a switching time period. The conversion rate of the inductor current for the current prediction method is as Equation (3).

$$\frac{d}{dt} I_{bat} \approx \frac{1}{T_S} \times e_i \tag{3}$$

where e_i represents the current error (e_i=I_{bat}*-I_{bat}) and T_s represents the switching time period.

Equation (4) shows the voltage of inductor L.

$$L\frac{d}{dt} I_{bat} = V_{bat} - (1 - d_{S1}) \times V_{bus} \tag{4}$$

Applying equation (3) to equation (4) will derive duty ratio of power semiconductor switch S_1, as shown in equation (5).

$$d_{S1} = 1 - \frac{1}{V_{bus}} \times \left(V_{bat} - \frac{L}{T_S} \times e_i \right) \tag{5}$$

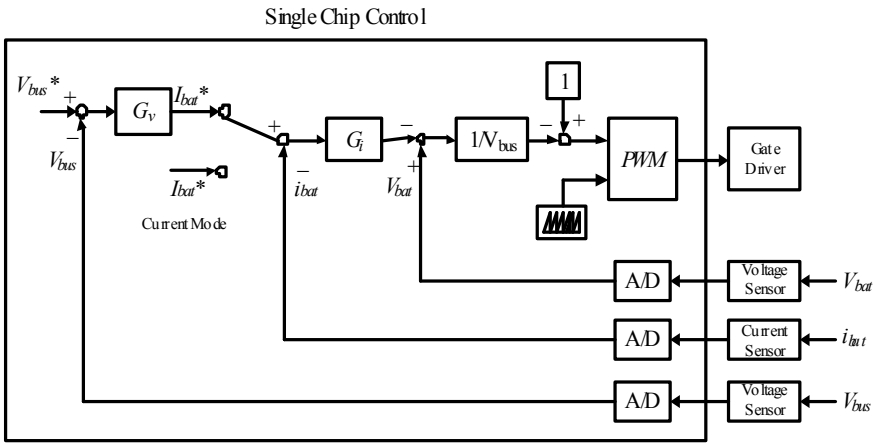

Fig. 5. Block diagram of bi-directional dc-dc converter.

A block diagram of a bi-directional dc-dc converter in boost mode can be derived, as shown in Fig. 5, according to equation (5). The bi-directional dc-dc converter of the lithium-ion battery adopts the constant-voltage control while the bi-directional dc-dc converter of the lead-acid batteries adopts the constant-current control

D. Control Method of Parallel Power Systems

This paper presents a set of lithium-ion batteries in parallel with *N* sets of lead-acid batteries to supply power. As an example, three sets of batteries in parallel are shown in Fig. 6. The No. 2 lead-acid battery supplies power first and then links with the No. 1 lead-acid battery for parallel operating. Finally, the lithium-ion battery operates in parallel with the two sets of lead-acid batteries. In this example, P0 is the power of the lithium-ion battery, P1 is the power of the No. 1 lead-acid battery, P2 is the power of the No. 2 lead-acid battery and P_{Load} is the load power of the electric vehicle. The operation modes of the parallel-battery power supply can be divided in six ways. To simplify the analysis, the power loss of the converters is ignored.

1) Discharge of No.2 lead-acid battery to the electric vehicle: first, the No. 2 lead-acid battery discharges alone. The output power of the No. 2 lead-acid battery equals the load power of the electric vehicle motor. Fig. 6(a) shows the power flows for the discharge of the No.2 lead-acid battery to the electric vehicle as $P2=P_{Load}$.

2) Power supply of No. 1 and No. 2 lead-acid batteries in parallel: after the No. 2 lead-acid battery is discharged corresponding to the load current until its output voltage drops to the cut-off voltage. The No. 1 and No. 2 lead-acid batteries in parallel are placed to supply power as $P1+P2=P_{Load}$. The No. 2 lead-acid battery cannot release power anymore and must stop discharging since it has reached the cut-off voltage. However, instead of the No. 2 lead-acid battery, a small discharge rate (1C ~ 0.1C) is set so that the No. 2 lead-acid battery will continue to supply power to increase the available capacity of the lead-acid battery. Fig. 6(b) shows the power flows for the power supply of the No.1 and No.2 lead-acid batteries in parallel.

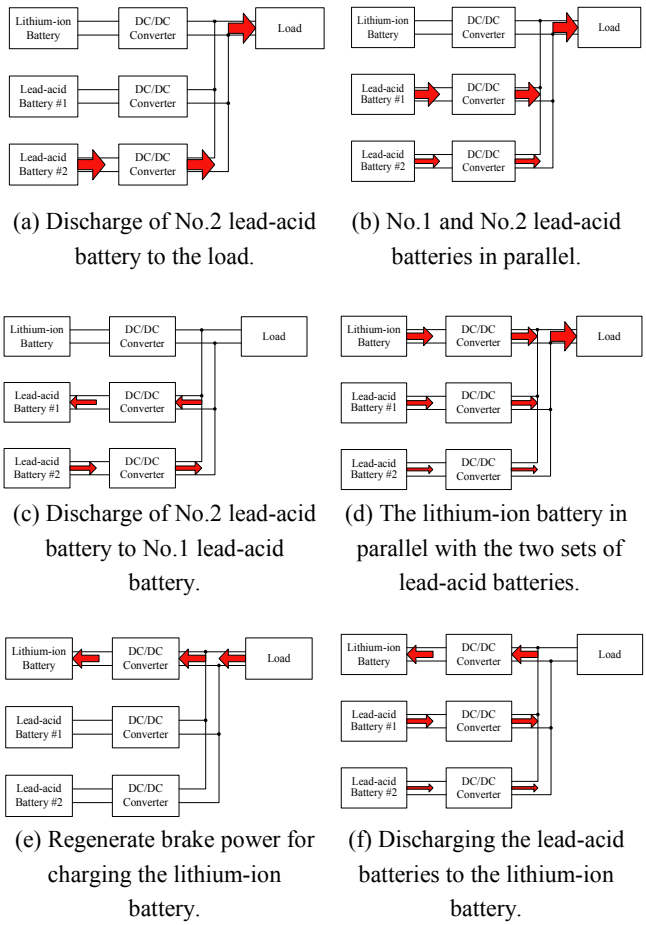

(a) Discharge of No.2 lead-acid battery to the load.

(b) No.1 and No.2 lead-acid batteries in parallel.

(c) Discharge of No.2 lead-acid battery to No.1 lead-acid battery.

(d) The lithium-ion battery in parallel with the two sets of lead-acid batteries.

(e) Regenerate brake power for charging the lithium-ion battery.

(f) Discharging the lead-acid batteries to the lithium-ion battery.

Fig. 6. Power flows in parallel for a set of lithium-ion battery and the two sets of lead-acid batteries.

3) Discharge of No.2 lead-acid battery to No.1 lead-acid battery: when the electric vehicle stops, the power demand of the electric vehicle motors is zero. However, to fully utilize the remaining energy in the No. 2 lead-acid battery, the No. 2 lead-acid battery continues discharging a small current (0.3C ~ 0.1C) to the output terminal to charge the No. 1 lead-acid battery. Thus the input power of the No. 2 lead-acid battery equals the output power of the No. 1 lead-acid battery. At this stage, the remaining energy of the No. 2 lead-acid battery will be transferred to the other batteries to increase their SOC, thereby improving the SOC of the electric vehicle batteries. Fig. 6(c) shows the power flows for the No.2 lead-acid battery discharging to the No.1 lead-acid battery.

4) Discharge of the lithium-ion battery in parallel with the two sets of lead-acid batteries: when the No. 1 lead-acid battery is discharged to the cut-off voltage, it is replaced by the lithium-ion battery in parallel with the two sets of lead-acid batteries for discharge in which the No. 1 lead-acid battery is replaced by a small discharge rate (1C ~ 0.1C). If there is energy remaining in the No. 2 lead-acid battery, the small current continues discharging from the No. 2 lead-acid battery until the discharge current drops to 0.1C and the cut-off voltage is reached as the internal energy of the No. 2 lead-acid battery is fully released. Fig. 6(d) shows the power flows for the discharge of the lithium-ion battery in parallel with the two sets of lead-acid batteries as P0+P1+P2= P_{Load}.

5) Regenerate brake power for charging the lithium-ion battery: when the electric vehicle is decelerating or going downhill, it can regenerate the brake power with a negative P_{Load}. The regenerated brake power will be stored in the lithium-ion battery to fully use the regenerated energy. Taking a Molicel IBR26700A lithium-ion battery as an example, the maximum charge current can be up to 3C. Regeneration must be combined with the lithium-ion battery capacity estimation system to prevent battery overcharge. When the regeneration is completely recharged back to the lithium-ion battery, the charge power of the lithium-ion battery equals the regeneration. Fig. 6(e) shows the power flows of the regeneration for charging the lithium-ion battery as P0 = $P_{Load.}$ If the brake regeneration current is greater than the maximum charge current of the lithium-ion battery, the excessive regenerated brake power is required to be consumed by the braking resistors to prevent over-voltage of the lithium-ion battery and burning or explosion hazards.

6) Discharging the lead-acid batteries to the lithium-ion battery: when the electric vehicle stops or reaches its destination, the lead-acid batteries still continuously discharge to the lithium-ion battery through a small current. At this time, the lithium-ion battery is in a charge state. Fully utilizing the remaining energy stored in the lead-acid batteries will benefit the return capability of the electric vehicle. Fig. 6(f) shows the power flows for the lead-acid batteries discharging to the lithium-ion battery.

IV. Experimental Results

This paper will use YUASA lead-acid batteries, CSB lead-acid batteries and GS lead-acid batteries for verifying the effectiveness of the proposed method. These lead-acid batteries are sealed, maintenance free batteries. This experiment used a set of lead-acid batteries and a set of Molicel IBR26700A (24V/5.6AH) lithium-ion battery packs, making a total of two sets of batteries operating in parallel. Of these, the lithium-ion battery packs were based on custom specifications.

Taking a Molicel IBR26700A as an example, the single cell specification was 3.75V/2.8AH with a gravimetric energy density of 105Wh/kg, a volumetric energy density of 270Wh/l, a battery voltage range of 2.5V~4.2V and a maximum output current of 40A. This experiment uses 14 cells in series-parallel connection in which seven cells are connected in series for two units and then the two units are combined in parallel to be a 24V/5.6AH lithium-ion battery pack.

To simplify the circuit, the bi-directional dc-dc converter of the lithium-ion battery is omitted. Thus the output terminal of the lithium-ion battery is connected to the load as the voltage of the output terminal is 24V. The lead-acid battery is based on commercial standards. The output voltage of each lead-acid battery is 12V and it rises to 24V through the bi-directional dc-dc converter, and then connects with the lithium-ion battery in parallel for operation.

A. Design of the Bi-directional DC-DC Converter

The specifications and parameter design of the bi-directional dc-dc converter are as follows: battery voltage 12V, output voltage 24V, battery output current 10A, switching frequency 20kHz, single chip PIC 16F877A, L = 0.75mH, C_1 = 4700uF/50V, C_2 = 2000uF/100V, MOSFET IRFP250.

1) One battery power supply to the load: The bi-directional dc-dc converter which operates in boost mode is to enable a constant output voltage at the V_{bus} side. Therefore, the dc-dc converter needs to be operated under voltage-mode control. In order to test the performance of the bi-directional dc-dc converter, a 48Ω-6Ω-48Ω variation of the load R is simulated. The waveform of the transient response of this bi-directional dc-dc converter output voltage V_{bus} and load current I_o is shown as Fig. 7. It reports 24V of output voltage V_{bus} and a 0.5A-4A-0.5A variation for the load current I_o. Fig. 8 shows the constant waveform of V_{GS} for the power MOSFET and the load current I_o. The load current I_o is 5A.

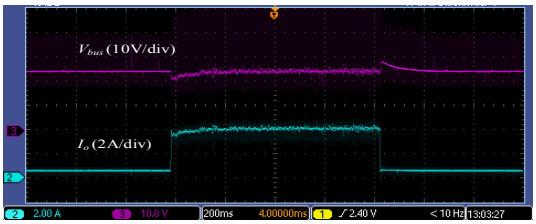

Fig. 7. Transient waveform of output voltage V_{bus} and load current I_0 for one battery operation.

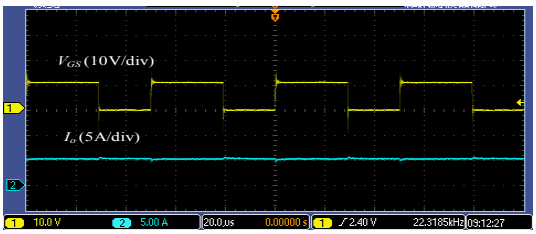

Fig. 8. Steady waveform of V_{GS} of power MOSFET and load current I_o.

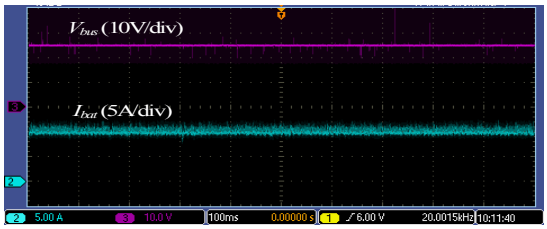

Fig. 9. Waveform of constant output current for lead-acid battery.

2) Experiments on the Parallel Batter: The output of the lithium-ion battery directly connects to the V_{bus} side and then to the loads. Therefore the voltage of the V_{bus} side is 24V. The output current of the lead-acid batteries is calculated via the single chip control core of the battery management systems to ensure that the lead-acid batteries discharge current to the V_{bus} side with a constant current. At this time, the bi-directional dc-dc converter of the lead-acid batteries operate by the current-mode control. This is accomplished by controlling the output current of the lead-acid batteries to achieve the current command I_{bat}^* of the battery management systems. Fig. 9 shows the waveform of the output current for the lead-acid batteries, in which the output current I_{bat} is 10A and the voltage of the V_{bus} side is 24V.

B. Releasable Capacity of the YUASA Lead-acid Battery Test

1) Discharging the lead-acid batteries to a load: YUASA NP5-12 12V/5AH lead-acid batteries provide power to the load. A two-stage current discharge is then applied to determine the releasable capacity under different loads for the lead-acid batteries. It is also used to calculate the releasable capacity by a small current discharge when the battery output voltage drops to the cut-off voltage. During the first stage, a constant discharge rate ranging from 0.5C to 2C is respectively applied to simulate the difference in power under load changes. The cut-off voltage of the lead-acid batteries is set at 10.5V. When the output voltage drops to 10.5V, the second stage starts and the output current is changed into a constant small current of 0.1C for discharge. The cut-off voltage in the second stage is also 10.5V.

Fig. 10(a) shows the profiles of the output voltage and the capacity of the batteries during the first stage of adopting a 0.5C constant discharge rate and during the second stage of using a 0.1C small discharge rate, where the released capacity is about 69% of the rated battery capacity in the first stage and about 23% in the second stage. Fig. 10(b) shows that the released capacity is about 60% in the first stage and about 31% in the second stage under a 1C-0.1C discharge rate. Fig. 10(c) shows that the released capacity is about 49% in the first stage and about 40% in the second stage under a 1.5C-0.1C discharge rate. Fig.10 (d) shows that the released capacity is about 38% in the first stage and about 48% in the second stage under a 2C-0.1C discharge rate.

Fig. 11 shows the release of different capacities under different discharge currents of the YUASA lead-acid batteries, where Q1 denotes the released capacity in the first stage and Q2 denotes the released capacity in the second stage. Experimental results indicate that the size of the battery discharge rate can significantly influence the releasable capacity to the extent that a larger discharge current leads to a failure to release more energy. The released capacity in the second stage is the exploitation power of the batteries studied in this paper. This portion of the power accounts for a large proportion of the capacity in lead-acid batteries. Effectively releasing it would significantly enhance the available capacity of electric vehicle batteries.

2) Discharging lead-acid batteries to a lithium-ion battery: It is assumed that lead-acid batteries discharge through 1.5C to the load. When its voltage drops to the cut-off voltage, a multi-stage small discharge current is used. The lead-acid batteries initially discharge through 1.0C to the output side. When the battery voltage drops to the cut-off voltage, the size of the discharge current is reduced. The batteries then change to a discharge rate of 0.8C until the battery voltage drops again to the cut-off voltage. At that time, the size of the discharge current can be reduced again and the steps continued repeatedly to reduce the discharge current by reducing 0.1~0.2C per stage until the discharge current drops to 0.1C and the battery voltage drops to the cut-off voltage. The SOC of the lithium-ion battery is set as 50% in advance and the above-energy charges lithium-ion battery.

Fig. 12 shows the parallel operation of YUASA lead-acid batteries and lithium-ion battery where the lead-acid batteries discharge to the lithium-ion battery. The solid line represents

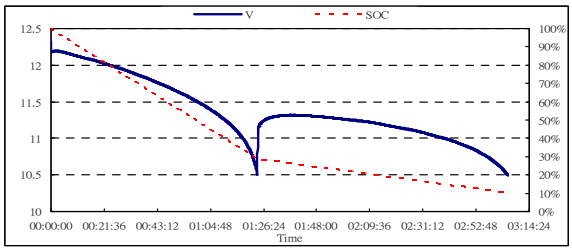

(a) 0.5C-0.1C.

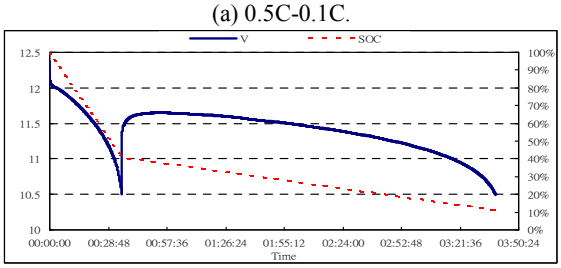

(b) 1.0C-0.1C.

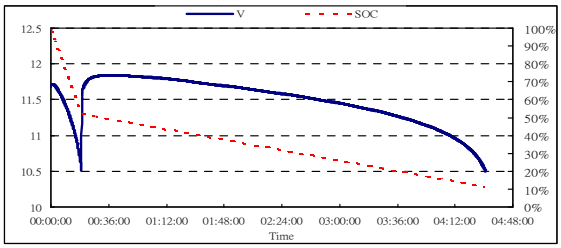

(c) 1.5C-0.1C.

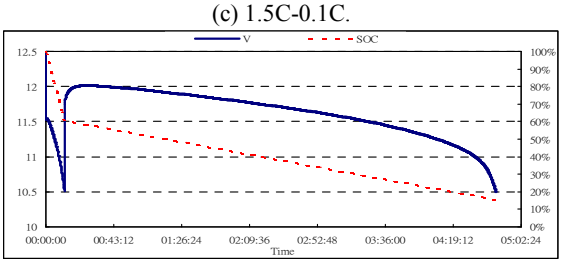

(d) 2C-0.1C.

Fig. 10. The profiles of the output voltage and capacity of the YUASA lead-acid battery for two-stage discharge currents.

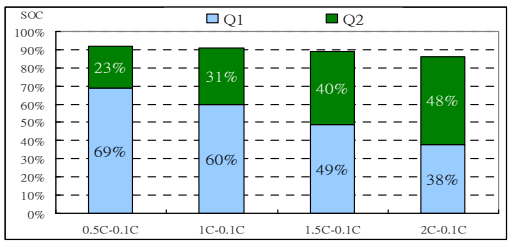

Fig.11. The released capacity under two-stage discharge currents for the YUASA lead-acid battery.

the lead-acid battery output voltage, and the dashed line represents the discharge current. The charge/discharge lasts about 1 hour and 39 minutes. Furthermore, the lithium-ion battery capacity increases 0.72AH/24V. Correspondingly, the capacity of the YUASA lead-acid batteries rises to 33% of the rated capacity.

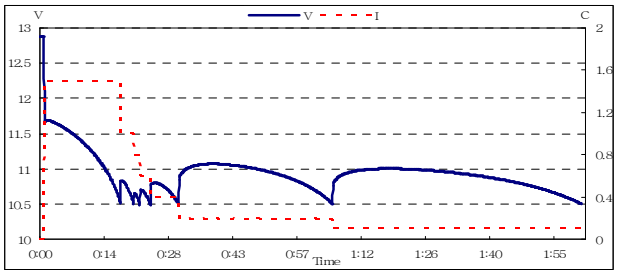

Fig. 12. The parallel operation of YUASA lead-acid battery and lithium-ion battery.

C. *Releasable Capacity of the CSB Lead-acid Battery Test*

Three sets of CSB lead-acid batteries (CSB GP1245 12V/4.5AH sealed lead-acid batteries) are used for the discharge test in this section. The test is based on the discharge program from the previous section. Fig. 13(a) shows the profiles of the output voltage and the capacity of the CSB lead-acid batteries in the first stage of adopting a 0.5C constant discharge rate and in the second stage of using a 0.1C small discharge rate, where the released capacity is about 75% of the rated battery capacity in the first stage and about 23% in the second stage. Fig. 13(b) shows that the released capacity is about 62% in the first stage and about 35% in the second stage under a 1C-0.1C discharge rate. Fig. 13(c) shows that the released capacity is about 51% in the first stage and about 44% in the second stage under a 1.5C-0.1C discharge rate. Fig. 13 (d) shows that the released capacity is about 40% in the first stage and about 53% in the second stage under a 2C-0.1C discharge rate.

Fig. 14 shows the released capacity under two-stage discharge currents for the CSB lead-acid batteries, where Q1 denotes the released capacity in the first stage and Q2 denotes the released capacity in the second stage.

The CSB lead-acid batteries are discharged by 1.5C initially. When the output voltage of lead-acid batteries drops to the cut-off voltage, a multi-stage small discharge current is adopted. Fig. 15 shows the profiles of the output voltage and the current under a multi-stage small discharge current for the CSB lead-acid batteries. The solid line represents the CSB lead-acid battery output voltage, and the dashed line represents the discharge current. Fig. 15(a) denotes CSB lead-acid battery #1. Fig. 15(b) denotes CSB lead-acid battery #2. Fig. 15(c) denotes CSB lead-acid battery #3. The available capacity of the three sets of lead-acid batteries was increased by an average of 40% of the rated capacity.

D. *Releasable Capacity of the GS Lead-acid Battery Test*

Three sets of GS lead-acid batteries (GS GTX5L-BS 12V/4AH sealed lead-acid batteries) were used for the discharge test in this section. The test is based on a discharge program from the previous section. Fig. 16(a) shows the profiles of the output voltage and the capacity of the GS

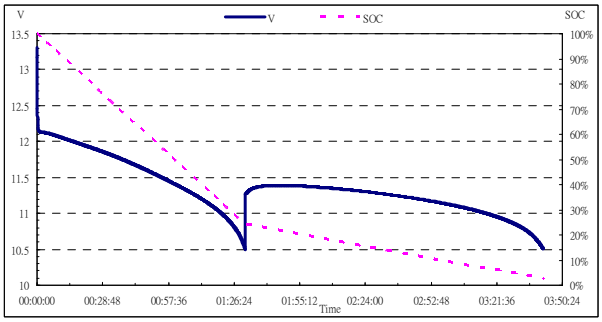

(a) 0.5C-0.1C.

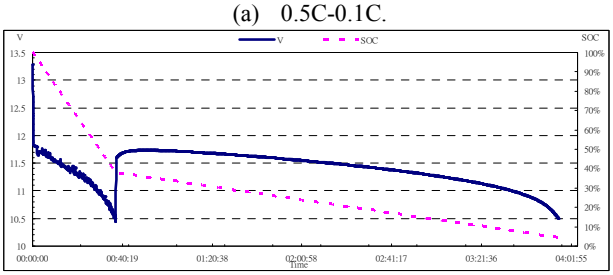

(b) 1C-0.1C.

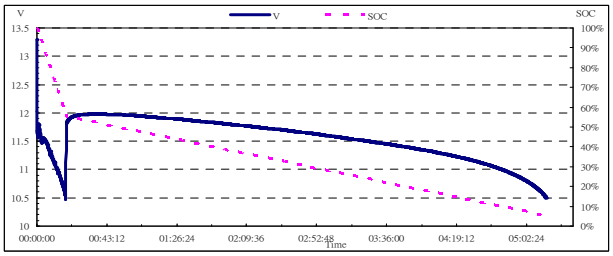

(c) 1.5C-0.1C.

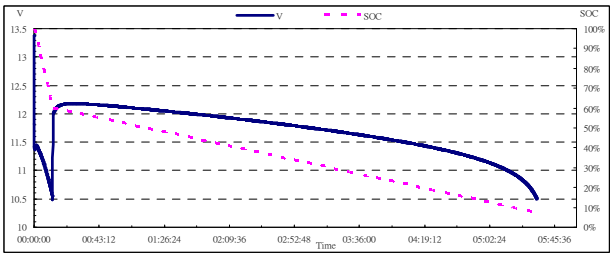

(d) 2C-0.1C.

Fig. 13. The profiles of the output voltage and capacity of the CSB lead-acid battery for two-stage discharge currents.

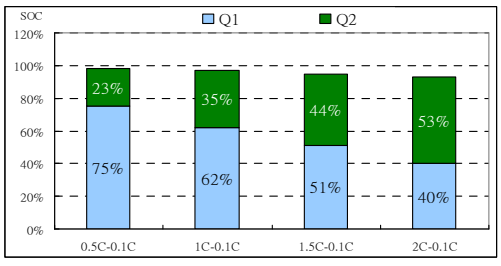

Fig. 14. The released capacity under two-stage discharge currents for CSB lead-acid battery.

lead-acid batteries in the first stage of adopting a 0.5C constant discharge rate and in the second stage of using a 0.1C small discharge rate, where the released capacity is

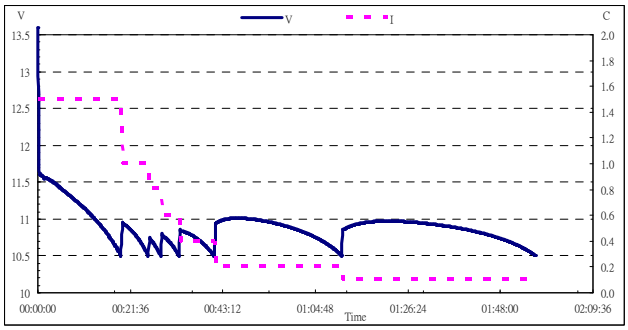

(a) CSB lead-acid battery #1

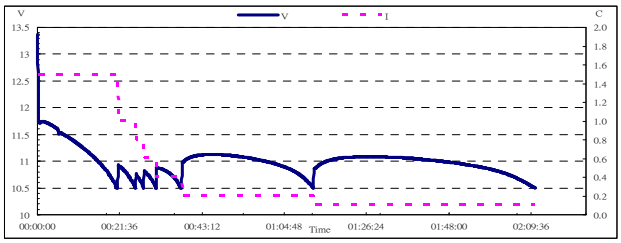

(b) CSB lead-acid battery #2

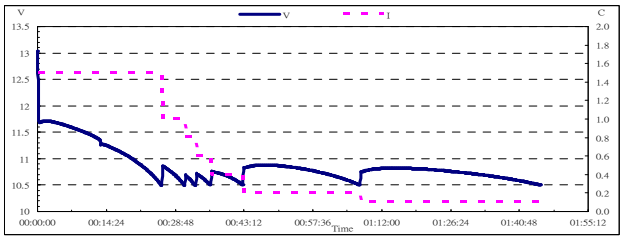

(c) CSB lead-acid battery #3

Fig. 15. The discharge profiles under a multi-stage small discharge current for CSB lead-acid battery.

about 83% of the rated battery capacity in the first stage and about 16% in the second stage. Fig. 16(b) shows that the released capacity is about 66% in the first stage and about 32% in the second stage under a 1C-0.1C discharge rate. Fig. 16(c) shows that the released capacity is about 61% in the first stage and about 37% in the second stage under a 1.5C-0.1C discharge rate. Fig.16 (d) shows that the released capacity is about 46% in the first stage and about 51% in the second stage under a 2C-0.1C discharge rate. Fig. 17 shows the release of different capacities under different discharge currents of the GS lead-acid batteries, where Q1 denotes the released capacity in the first stage and Q2 denotes the released capacity in the second stage.

Fig. 18 shows the profiles of the output voltage and the current under a multi-stage small discharge current for the GS lead-acid batteries, where the solid line represents the GS lead-acid battery output voltage and the dashed line represents the discharge current. Fig. 18(a) denotes GS lead-acid battery #1. Fig. 18(b) denotes GS lead-acid battery #2. Fig. 18(c) denotes GS lead-acid battery #3.

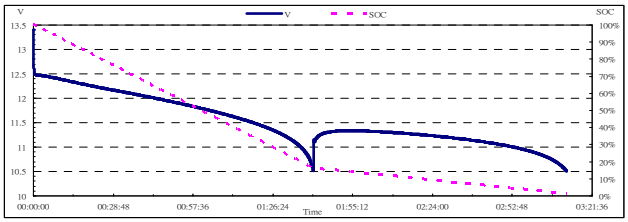

(a) 0.5C-0.1C

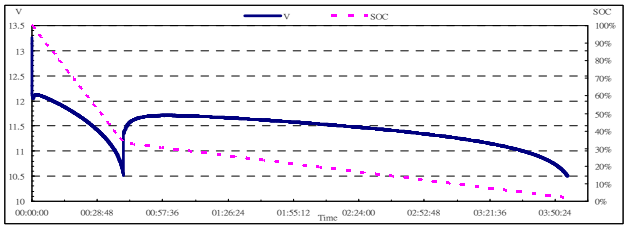

(b) 1C-0.1C

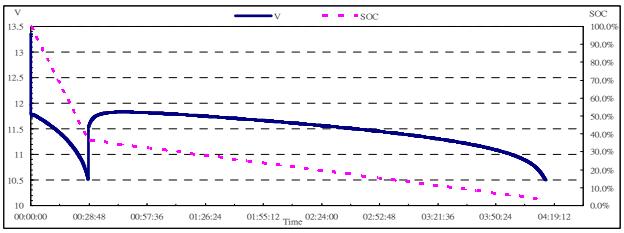

(c) 1.5C-0.1C

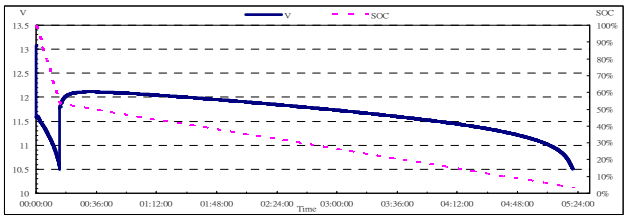

(d) 2C-0.1C

Fig. 16. The profiles of the output voltage and capacity of the GS lead-acid battery for two-stage discharge currents.

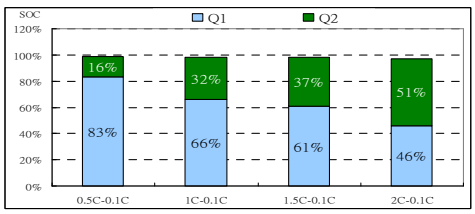

Fig. 17. The released capacity under two-stage discharge currents for GS lead-acid battery.

Fig. 19 shows the release capacity of a GS lead-acid battery under a multi-stage small discharge current, where Q1 denotes the released capacity in the first stage and Qn denotes the released capacity of the multi-stage small current. The available capacity of lead-acid battery #1 was increased by 34% of the rated capacity, that of battery #2 was increased by 34%, and that of battery #3 was increased by 38%. The available capacities of these lead-acid batteries were increased by an average of 35.3% of the rated capacity.

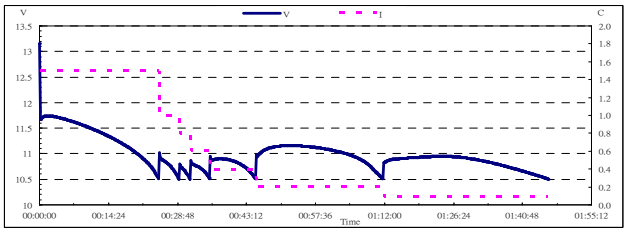

(a) GS lead-acid battery #1

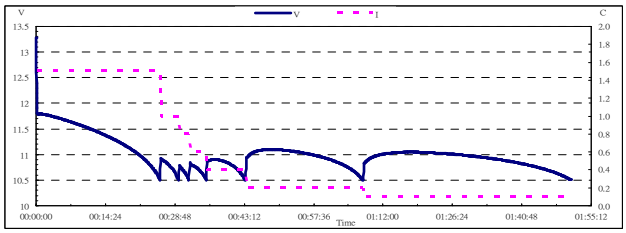

(b) GS lead-acid battery #2

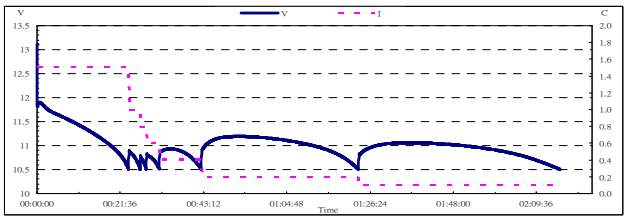

(c) GS lead-acid battery #3

Fig. 18. The discharge profiles under a multi-stage small discharge current for GS lead-acid battery.

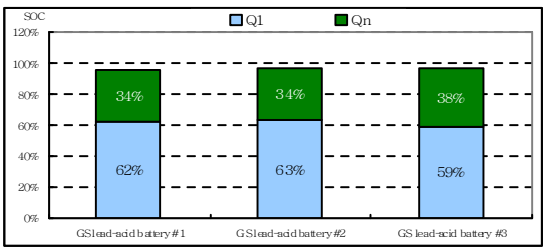

Fig. 19. The release capacity under a multi-stage small discharge current for GS lead-acid battery.

V. CONCLUSIONS

This paper uses a set of lithium-ion batteries and *N* sets of lead-acid batteries in parallel. First, the lead-acid batteries provide power. When the lead-acid batteries discharge to the cut-off voltage, a multi-stage small current continues to discharge. These batteries can provide power for part of the load or charge the lithium-ion battery until all of the stored energy of the lead-acid batteries is fully released. Through the multi-stage small current discharge of the lead-acid batteries and efficient utilization of the electric vehicle usage features, the un-released energy of the lead-acid batteries can be fully utilized during the waiting time before the electric vehicle's return. This paper used YUASA lead-acid batteries, CSB lead-acid batteries and GS lead-acid batteries for verifying the effectiveness of the proposed method.

The experimental results demonstrate that the proposed control methods can significantly increase the available capacity of the lead-acid batteries. As the load current increases, its effect becomes more obvious. When the load current is 0.5C, the available capacity of the lead-acid batteries is 75% of the rated capacity without control and 96% of the rated capacity for the proposed control methods. When the load current is 1C, the available capacity of the lead-acid batteries is 63% of the rated capacity without control and 95% of the rated capacity for the proposed control methods. When the load current is 1.5C, the available capacity of the lead-acid batteries is 54% of the rated capacity without control and 94% of the rated capacity for the proposed control methods. When the load current is 2C, the available capacity of the lead-acid batteries is 41% of the rated capacity without control and 92% of the rated capacity for the proposed control methods.

REFERENCES

[1] D. Somayajula, A. Meintz, and M. Ferdowsi, "Study on the effects of battery capacity on the performance of hybrid electric vehicles," *IEEE Vehicle Power and Propulsion Conference (VPPC)*, pp. 1-5, Sep. 2008.

[2] S. B. Han, M. L. Jeong, S. M. Hyung, and H. C. Gyu, "Load sharing improvement in parallel-operated lead acid batteries," in *Proc IEEE ISIE'01*, Vol. 2, pp. 1026-1031, Jun. 2001.

[3] L. Benini, D. Bruni, A. Macii, E. Macii, and M. Poncino, "Discharge current steering for battery lifetime optimization," *IEEE Trans. Computer*, Vol. 52, No.8, pp. 985-995, Aug. 2003.

[4] L. Benini, A. Macii, E. Macii, M. Poncino, and R. Scarsi, "Scheduling battery usage in mobile systems," *IEEE Trans. VLSI*, Vol. 11, No. 6, pp. 1136-1143, Dec.2003.

[5] C. S. Moo, K. S. Ng, and Y. C. Hsieh, "Parallel operation of battery power modules," *IEEE Trans. Energy Convers.*, Vol. 23, No. 2, pp. 701-707, Jun. 2008.

[6] *http://www.csb-battery.com*, Aug. 2012.

[7] *http://www.molicel.com*, Aug. 2012.

[8] E. Karden, S. Ploumen, B. Fricke, T. Miller, and K. Snyder, "Energy storage devices for future hybrid electric vehicles," *J. Power Sources*, Vol. 168, pp.2-11, May 2007.

[9] O. Coumont, P. Le Moigne, C. Rombaut, X. Muneret and P. Lenain, "Enery gauge for lead-acid batteries in electric vehicles," *IEEE Trans. Energy Convers.*, Vol. 15, No. 3, pp. 354-360, Sep. 2000.

[10] M. Ceraolo and G. Pede, "Techniques for estimating the residual range of an electric vehicle," *IEEE Trans. Veh. Technol.*, Vol. 50, No. 1, pp. 109-115, Jan. 2001.

[11] P. Sabine, P. Marion, and A. Jossen, "Methods for state-of-charge determination and their applications," *J. Power Sources*, Vol. 96, No. 1, pp. 113-120, Jun. 2001.

[12] M. Coleman, C. K. Lee, C. Zhu, and W. G. Hurley, "State-of-charge determination from EMF voltage estimation using impedance, terminal voltage, and current for lead-acid and lithium-ion batteries," *IEEE Trans. Ind. Electron.*, Vol. 54, No. 5, pp. 2550-2557, Oct. 2007.

[13] F. Pei, K. Zhao, Y. Luo, and X. Huang, "Battery variable current-discharge resistance characteristics and state-of-charge estimation of electric vehicle," in *Proc. IEEE WCICA'06*, Vol. 2, pp. 8314-8318, Jun. 2006.

[14] O. Tremblay, L. A. Dessaint, and A. I. Dekkiche, "A generic battery model for the dynamic simulation of hybrid electric vehicles," *IEEE Vehicle Power and Propulsion Conference, VPPC*, pp.284-289, Sep. 2007.

[15] M. Jain, M. Daniele, and P. K. Jain, "A bi-directional dc-dc converter topology for low power application," *IEEE Trans. Power Electron.*, Vol. 15, No. 4, pp.595-606, 2000.

[16] K. Wang, C. Y. Lin, L. Zhu, D. Qu, F. C. Lee, and J. S. Lai, "Bi-directional dc to dc converters for fuel cell system," *IEEE Power Electronics in Transportation*, pp.47-51, 1998.

[17] J.N. Marie-Francoise, H. Gualous and A. Berthon, "DC to DC converter with neural network control for on-board electrical energy management," in *Proc. IEEE IPEMC, Belfort, France*, pp.521-525, Aug. 2004.

[18] K. Jin, X. Ruan, M. Yang, M. Xu, "A hybrid fuel cell power system," *IEEE Trans. Ind. Electron.*, Vol. 56, No. 4, pp. 1212-1222, Apr. 2009.

Yow-Chyi Liu was born in Kaohsiung, Taiwan ROC. He received his M.S. and Ph.D. in Electrical Engineering from the National Chen Kung University, Tainan, Taiwan ROC, in 1994, and 2005, respectively. He is currently an Assistant Professor in the Department of Electrical Engineering, Kao Yuan University, Kaohsiung City, Taiwan ROC. His current research interests include power electronics, electric vehicles, batteries, and rapid transit systems.